GABAergic synaptic scaling in embryonic motoneurons is mediated by a shift in the chloride reversal potential

Carlos E Gonzalez Islas, *Emory University*
Nikolai Chub, *National Institutes of Health*
Miguel Angel Garcia-Bereguiain, *Emory University*
Peter Wenner, *Emory University*

Journal Title: Journal of Neuroscience Nursing
Volume: Volume 30, Number 39
Publisher: Society for Neuroscience | 2010-09-29, Pages 13016-13020
Type of Work: Article | Post-print: After Peer Review
Publisher DOI: 10.1523/JNEUROSCI.1659-10.2010
Permanent URL: http://pid.emory.edu/ark:/25593/cr745

Final published version:
http://dx.crossref.org/10.1523/JNEUROSCI.1659-10.2010

Published in final edited form as:
J Neurosci. 2010 September 29; 30(39): 13016–13020. doi:10.1523/JNEUROSCI.1659-10.2010.

GABAergic synaptic scaling in embryonic motoneurons is mediated by a shift in the chloride reversal potential

Carlos Gonzalez-Islas
Department of Physiology, Room 601, Whitehead Bldg., Emory University, School of Medicine, Atlanta, GA, 30322

Nikolai Chub
Developmental Neurobiology Section, NINDS, NIH Building 35, Room 3C-712 35 Convent Drive Bethesda, MD 20892-3721

Miguel Angel Garcia-Bereguiain
Department of Physiology, Room 601, Whitehead Bldg., Emory University, School of Medicine, Atlanta, GA, 30322

Peter Wenner*
Department of Physiology, Room 601, Whitehead Bldg., Emory University, School of Medicine, Atlanta, GA, 30340

Abstract

Homeostatic synaptic plasticity ensures that networks maintain specific levels of activity by regulating synaptic strength in a compensatory manner. When spontaneous network activity (SNA) was blocked *in vivo* in the embryonic spinal cord, compensatory increases in excitatory GABAergic synaptic inputs were observed. This homeostatic synaptic strengthening was observed as an increase in the amplitude of GABAergic miniature postsynaptic currents (mPSCs). We find that this process is mediated by an increase in chloride accumulation which produces a depolarizing shift in the GABAergic reversal potential (E_{GABA}). The findings demonstrate a previously unrecognized mechanism underlying homeostatic synaptic scaling. Similar shifts in E_{GABA} have been described following various forms of neuronal injury, introducing the possibility that these shifts in E_{GABA} represent a homeostatic response.

Keywords

spinal cord; development; GABA; synaptic plasticity; $GABA_A$ receptor; motoneuron

Introduction

Homeostatic synaptic plasticity is the process of homeostatically maintaining network activity levels through compensatory adjustments in synaptic strength (Rich and Wenner, 2007; Turrigiano, 2008). For example, when network activity was blocked in cultured neural networks for days, increases in the amplitude of excitatory mPSCs, and decreases in the amplitude of inhibitory GABAergic mPSCs were observed (Kilman et al., 2002; Turrigiano et al., 1998). The compensatory changes in mPSC amplitude were observed throughout the distribution of amplitudes (synaptic scaling (Turrigiano et al., 1998)). The mechanisms that underlie compensatory changes in excitatory and inhibitory quantal amplitude following

*Corresponding Author: Phone (404) 727-1517 Fax (404) 727-2648 pwenner@emory.edu.

activity blockade of cultured networks include changes in postsynaptic receptor number and the amount of transmitter released per vesicle (Rich and Wenner, 2007; Turrigiano, 2008; Wilson et al., 2005). Mechanisms underlying synaptic scaling following activity perturbations *in vivo* are poorly understood.

We have recently identified homeostatic synaptic scaling in the embryonic network (Gonzalez-Islas and Wenner, 2006). Spontaneous network activity (SNA) is observed in virtually all developing circuits, and is thought to be important for the maturation of the synaptic networks in which it is expressed (Ben-Ari, 2001; O'Donovan, 1999; Zhang and Poo, 2001). In the spinal cord, SNA occurs as episodes of activity experienced in most cells, followed by longer duration periods of inactivity (O'Donovan et al., 1998). Spinal SNA, observed through embryonic movements, was blocked in the chick embryo *in ovo*, which resulted in GABAergic synaptic scaling in motoneurons. An increase in $GABA_A$ mPSC amplitude was compensatory because of the depolarizing nature of GABA at this stage of development (Gonzalez-Islas and Wenner, 2006). In the current study we demonstrate an increase in the driving force for GABAergic currents, but find no evidence for an increase in postsynaptic $GABA_A$ receptors or vesicle content of GABA. This change in E_{GABA} was mediated by an increase in chloride accumulation.

Methods

Dissection

Stage 36 (Hamburger and Hamilton, 1951) chick embryo spinal cords, with attached muscle nerves, were dissected under cooled (15°C) Tyrode's solution containing (in mM): 139 NaCl, 12 D-glucose, 17 $NaHCO_3$, 3 KCl, 1 $MgCl_2$, and 3 $CaCl_2$ (full description - (Gonzalez-Islas and Wenner, 2006). After the dissection, the cord was allowed to recover for at least 6 hours in Tyrode's at 18°C. The cord was then transferred to a recording chamber, continuously perfused with Tyrode's solution that was heated to 28°C.

mPSC recordings

Whole cell patch-clamp recordings were made from ventral horn motoneurons localized between the lumbosacral segment 1 and 3 in order to acquire mPSCs, as described previously (Gonzalez-Islas et al., 2009). Briefly, whole cell recordings (electrodes, 5–10 MΩ) were obtained from antidromically identified motoneurons. Recordings were terminated whenever significant increases in input resistance (> 20%) occurred. Standard extracellular recording solution for mPSCs contained the following (in mM): NaCl, 139; KCl, 5; $NaHCO_3$, 17; $CaCl_2$, 3; $MgCl_2$, 1; D-glucose, 12; TEA, 30; CsCl, 5; TTX, 0.001. Glutamatergic antagonists CNQX (10μM) and AP-5 (50μM) were added to the bath to isolate GABAergic mPSCs. The intracellular patch solution for GABA mPSC recordings contained the following (in mM): 5 NaCl, 100 K-gluconate, 30 KCl, 5 CsCl, 10 TEA-Cl, 10 HEPES, 10 BAPTA, 1 $MgCl_2$, 0.1 $CaCl_2$, 1 Na_2ATP, and 0.1 MgGTP, 10 QX314 and 0.1 verapamil; pH was adjusted to 7.3 with KOH. Pipette solution osmolarity was between 280 and 300mOsm. Junction potentials were corrected online. Currents were filtered on-line at 5 kHz, digitized at 10 kHz, and analyzed using Minianalysis software (Synaptosoft, Inc.).

For experiments in 0mM HCO_3^-, I_{mPSC}-V data were collected in standard extracellular solution, then the solution was changed to a 0mM HCO_3^- extracellular solution, in which $NaHCO_3$ was substituted by 17 mM Na-gluconate and 10 mM HEPES; pH adjusted to 7.3 with NaOH. Additionaly the 0mM HCO_3^- solution was bubbled with 100% O_2. Pippette solution was (in mM) 5 Na-gluconate, 130 K-gluconate, 5 CsCl, 10 TEA-Cl, 10 HEPES, 10 BAPTA, 1 $MgCl_2$, 0.1 $CaCl_2$, 1 Na_2ATP, and 0.1 MgGTP, 10 QX314 and 0.1 verapamil; pH was adjusted to 7.3 with KOH.

Chloride leak recordings

For recording chloride leak conductances, we used the following external solution (in mM): 110 NaCl; 29 Na-gluconate; 17 $NaHCO_3$; 3 $CaCl_2$; 1 $MgCl_2$; 12 D-glucose; 30 TEA-Cl; 5 CsCl; 0.4 $CdCl_2$; 5 4-AP; 0.01 CNQX; 0.05 APV; 0.001 TTX. Pipette solution contained (in mM): 146 CsCl, 10 HEPES, 5 EGTA, 2 $MgCl_2$, 0.1 $CaCl_2$, 1 Na_2ATP, 0.5 MgGTP, 10 QX-314, and 0.1 verapamil; pH was adjusted to 7.3 with CsOH. The stimulus protocol employed to elicit this conductance, consisted of a voltage ramp from the holding potential of 0 mV to −90 mV, at a rate of 0.18 mV/ms.

Perforated patch recordings

Pipette solution for gramicidin perforated patch measurements contained (in mM): 140 K-gluconate, 10 NaCl, 10 HEPES and 30 sucrose, pH was adjusted to 7.2 with NaOH (detailed methods provided - (Chub and O'Donovan, 2001)). Gramicidin (from Bacillus brevis, Sigma-Aldrich) was added to pipette solution (final concentration 50 mg/ml). Seal and patch perforation took 30–50 min, and was made in normal Tyrode's solution, which was then replaced with bath solution containing (in mM): 139 NaCl, 5 KCl, 17 $NaHCO_3$, 1 $MgCl_2$, 12 glucose, 0.5 $MnCl_2$, 10 TEA-Acetate, 5 CsCl and 0.0005 TTX. Isoguvacine (100 μM) was dissolved in modified bath solution and locally applied with a pipette by a pressure pulse (15 psi, 20–40 sec) delivered with a picospritzer (General Valve Corp). The pipette was inserted in the ventral horn approximately 200–400μm from the recorded neurons. Liquid junction potential (−14.4 mV) was calculated using pClamp 9 and was corrected.

Pharmacology

At E8 lidocaine hydrochloride aqueous solution (35 mg/ml plus 10 mM HEPES, pH 7.2) was continuously applied onto the chorioallantoic membrane of the embryos at a rate of 13.5 ml/hr, as described previously (Gonzalez-Islas and Wenner, 2006); control embryos did not receive saline injections, as no difference was observed between untreated and saline-treated embryos in this previous study. Verapamil was purchased from Calbiochem; TTX, APV, and CNQX, were purchased from Tocris Cookson; CsCl was purchased from Fisher Scientific; BAPTA was purchased from Fluka; HEPES from Acros Organics. All other chemicals and drugs were purchased from Sigma-Aldrich.

Immunoblot

Ventral half lumbosacral spinal cords were homogenized in RIPA buffer supplemented with protease and phosphatase inhibitors (Sigma-Aldrich). Samples were then centrifuged at 16000g for 5 min to remove cell debris. Protein concentration was quantitated using Bradford reagent (Sigma-Aldrich). Samples were separated on 4–15% SDS-PAGE, and blotted to a nitrocellulose membrane. The primary antibodies to $GABA_A$ subunits were from Millipore and diluted 1:200 (rabbit anti-α1, 06-868, MW 51kDa; mouse anti-β2/3, MAB341, 55kDa), and to actin (mouse anti-actin from Sigma-Aldrich, dilution 1/10000). The secondary antibodies used were HRP-goat anti-mouse IgG (dilution 1/4000) and HRP-goat anti-rabbit IgG (dilution 1/2000) from Millipore. Primary antibodies to a receptor subunit and actin were co-applied (2 blots) or were applied separately (3 blots). The blot was visualized by ECL chemiluminescence (GE Healthcare). Quantitative analysis of protein expression was carried out by drawing boxes around the protein bands and normalizing the signal intensity to actin intensity using Image J (NIH). Blots were done 5 times, and each sample represents a lysate of 2–3 different cords.

Statistics

Data are expressed as mean ± standard error. Most statistical analysis was performed using a two-tailed Student's t-test (paired and unpaired) unless mentioned otherwise. GraphPad Instat software and Sigma Plot 9 were used for statistical analysis.

Results

GABAergic scaling was not mediated by increased conductance

Activity-blockade triggers synaptic scaling of GABAergic mPSCs (Gonzalez-Islas and Wenner, 2006). We confirmed these results by treating chick embryos with lidocaine (blocker of voltage-gated Na^+ channels) from embryonic day 8 to 10 (E8 – E10) to block SNA. We then isolated spinal cords at E10, and obtained whole cell recordings from antidromically-identified spinal motoneurons. Consistent with previous results we found an increase in GABAergic mPSC amplitude in activity-blocked motoneurons compared to controls (held at −70mV - control 11.3 ± 0.6pA, n=10, lidocaine-treated 17.4 ± 0.8pA, n=13; $p<0.0001$; Figure 1A; (Gonzalez-Islas and Wenner, 2006)). Several previous studies have shown that GABAergic and AMPAergic synaptic scaling were mediated by changes in postsynaptic receptor number, so we initially tested this idea by measuring protein levels for 2 $GABA_A$ subunits (α1, β2/3) that were expressed in the ventral half of the spinal cord. Western blots demonstrated no difference in protein levels in control and treated cords (Figure 1B; α1 - n=5 & p=1.0, β2/3 - n=5 & p=0.34, Mann Whitney Test). Increases in $GABA_A$ receptor function (receptor number, state of phosphorylation) or presynaptic vesicle GABA concentration would increase the conductance of the GABAergic mPSCs.

In order to test whether reducing activity *in ovo* leads to changes in $GABA_A$ mPSC conductance we constructed I_{mPSC}-V plots of GABAergic mPSCs as described previously (Gonzalez-Islas et al., 2009). Voltage-gated channels and glutamatergic transmission were blocked to isolate GABAergic mPSCs, which were typically recorded in voltage steps of 10mV (acquire ≥ 50 mPSCs, 1–2 minutes at each step, Figure 2A). We then took the average mPSC amplitude from each step and constructed I_{mPSC}-V plots. $GABA_A$ mPSC conductance (slope of I_{mPSC}-V plot) of activity-blocked motoneurons was not significantly different than controls (control 277.2 ± 9.0 pS, n=11; lidocaine-treated 296.3 ± 13.1 pS, n=16; p=0.29; Figure 2B–C). The results demonstrate that increases in the function of postsynaptic receptors or vesicular GABA concentration did not mediate GABAergic scaling following *in vivo* activity-blockade in embryonic motoneurons.

GABAergic scaling was produced by a depolarizing shift in $GABA_A$ reversal potential

I_{mPSC}-V plots demonstrated that the GABAergic reversal potential (E_{GABA}) had shifted to a significantly more depolarized level ($p < 0.0001$). Average E_{GABA} was −26.9 ± 1.0 mV for control, but −9.9 ± 1.1 mV in activity-blocked motoneurons (Figure 2B–C). This suggested that there was an increase in the driving force for these currents. We have previously shown that whole cell electrodes with 50mM chloride patch solutions (Nernst equation predicts ~ −30mV) can be used to measure E_{GABA} (Gonzalez-Islas et al., 2009).

To confirm these striking results we also used perforated patch recordings to measure E_{GABA}. We locally applied the $GABA_A$ receptor agonist, isoguvacine (100μM), in the motor column and currents were recorded in motoneurons (Figure 3). Extracellular Tyrodes solution was in the bath with various blockers to isolate $GABA_A$ currents (see Methods). The I–V plots were generated from currents recorded in response to voltage ramps made before and during isoguvacine application. The current measured before the isoguvacine puff, was then subtracted from that during the isoguvacine puff to create the $GABA_A$ I–V plot shown on the right of Figure 3, and the reversal potentials were determined (see

Methods and (Chub and O'Donovan, 2001)). Again, we found that E_{GABA} was significantly more positive in lidocaine-treated vs. control motoneurons ($p = 0.001$). Mean E_{GABA} was -37.9 ± 1.0 mV (n=7) in control motoneurons vs. -15 ± 3.1 mV (n=7) in activity-blocked motoneurons (Figure 3). On the other hand the conductance of the isoguvacine-evoked currents were slightly reduced (3.4 ± 0.5 nS for lidocaine-treated and 4.9 ± 0.4 nS for control motoneurons, $p = 0.04$). Collectively, these results demonstrate that a change in the driving force for GABA-mediated currents produced the upward scaling of GABAergic mPSCs following activity blockade.

Elevated Cl^-_{in} underlies the depolarized shift of E_{GABA}

We tested the possibility that activity-blocked motoneurons exhibit an increase in the permeability of HCO_3^- through $GABA_A$ receptor channels, as this would lead to a depolarizing shift in E_{GABA}. I_{mPSC}-V plots were generated for activity-blocked embryos to determine E_{GABA} in control solution (17mM HCO_3^-) and then following perfusion of a 0mM HCO_3^- extracellular solution (HEPES added and bubbled with 100% O_2) for 20 minutes (Figure 4A). This short term removal of extracellular HCO_3^- should significantly alter E_{GABA} if the permeability of the ion through the $GABA_A$ receptor had increased in activity-blocked embryos. Reducing HCO_3^- produced a small hyperpolarization of E_{GABA} that was not significant (E_{GABA} moved from -8.8 ± 2.8mV to -12.5 ± 3.0mV in the 0mM HCO_3^- solution, n=4, p=0.38). Reducing HCO_3^- did not significantly alter mPSC conductance (339 ± 21pS versus 314 ± 14pS, n=4, p=0.13). This result is similar to the small shift in E_{GABA} that was reported for control embryos, and may result from the reduced function of the anion exchanger, AE3, which also contributes to chloride accumulation (Gonzalez-Islas et al., 2009). These results suggest that changes in HCO_3^- permeability do not produce the depolarized shift in E_{GABA}, but suggest that elevated intracellular chloride levels produce the scaling of $GABA_A$ mPSCs in activity-reduced embryos.

Leak chloride current is not significantly reduced in lidocaine-treated embryos

Elevated Cl^-_{in} levels could occur through changes in the function of Cl^- transporters and/or through a reduction in Cl^- leak currents. Tonically active $GABA_A$ receptors and other non-ligand gated Cl^- channels contribute to the total Cl^- leak of the cell. To assess overall Cl^- leak we isolated these currents, to the extent possible in the isolated spinal preparation, by adding K^+, Ca^{2+}, Na^+ channel blockers, glutamatergic receptor blockers, and replacing K^+ with Cs^+ in intracellular and extracellular solutions (see Methods). We then recorded whole cell, from motoneurons and made voltage ramps from a holding potential of 0mV to -90mV. In order to maintain stable intracellular Cl^- levels at a holding potential of 0mV we set the chloride reversal potential near 0mV by using high concentrations of Cl^- in the extracellular and patch solutions. This also provided the advantage that the Cl^- leak current would have a significant driving force at voltages near the normal resting membrane potential, and could therefore be easily measured. Further, it was necessary to use high intracellular patch Cl^- to ensure that we set Cl^-_{in} (Gonzalez-Islas et al., 2009). We then constructed I–V plots to determine the conductance of the Cl^- leak in control and lidocaine-treated motoneurons (Figure 4B). We found a linear I–V relationship when we fit values between -90mV and -50mV (Figure 4B), typical of the resting membrane potential in these cells (Gonzalez-Islas and Wenner, 2006). Extension of the linear part of the fit allows us to approximate the reversal potential to 0 mV (control +1.9mV, lidocaine-treated +5.5mV), consistent with that expected for a chloride current. No significant difference ($p=0.72$) in the conductance of the leak current could be detected in control (1.45 ± 0.3nS, n=8) vs. activity-blocked embryos (1.25 ± 0.2nS, n=8), consistent with the idea that changes in Cl^- leak conductance did not underlie the greater Cl^- accumulation of the lidocaine-treated embryos. An outward current was activated above -40mV, and we suspect this was a cesium-mediated current passing through incompletely blocked voltage-gated calcium channels

(Hess et al., 1986). While we do not rule out the possibility there may also be a small reduction in conductance, it cannot account for the observed chloride accumulation in activity-blocked embryos. These results suggest that there is a positive shift in E_{GABA} that results from an increase in intracellular Cl^- accumulation, but not through a reduction in the Cl^- leak.

Discussion

Mechanisms underlying synaptic scaling have been studied almost exclusively following activity perturbations *in vitro*, and are thought to involve modifications that would change synaptic conductance. We show that $GABA_A$ mPSC conductance did not increase in activity-blocked embryonic motoneurons, demonstrating that there were no functional increases in postsynaptic receptors or vesicular transmitter concentration. In perforated patch recordings we actually saw a slight reduction in the $GABA_A$ agonist-evoked conductance in lidocaine-treated motoneurons. This change in conductance may have resulted from a modification of the extrasynaptic $GABA_A$ receptor population. Instead, we find a novel intuitive mechanism for synaptic scaling *in vivo*, where GABAergic scaling was mediated by an increase in the driving force for chloride-mediated currents. $GABA_A$ mPSC amplitudes increase by about 50% following *in ovo* activity-block in embryonic motoneurons. We show that activity blockade triggered a ~20mV depolarized shift in E_{GABA} using whole cell and perforated patch recordings. The depolarized shift in E_{GABA} was mediated by increases in intracellular chloride; HCO_3^- did not significantly influence E_{GABA} in control (Gonzalez-Islas et al., 2009) or lidocaine-treated embryos (Figure 4). Because Cl^- leak current was no different in control and activity-blocked motoneurons, it is likely that there is an increase in chloride accumulation in embryonic motoneurons. NKCC1 is thought to accumulate chloride beyond its passive distribution resulting in depolarizing GABAergic responses in the early development of many neurons (Ben-Ari et al., 2007; Blaesse et al., 2009). In embryonic motoneurons both NKCC1 and the anion exchanger, AE3, have been shown to accumulate chloride (Chub et al., 2006; Delpy et al., 2008; Gonzalez-Islas et al., 2009; Vinay and Jean-Xavier, 2008), and are therefore likely candidates for mediating the enhanced Cl^-_{in} in activity-blocked motoneurons.

Recent work has raised the possibility that the depolarized nature of GABA, and the resulting spontaneous network activity observed *in vitro* in neonatal brain slices were a consequence of saline solutions that were deficient in energy substrates, such as ketone bodies (Holmgren et al., 2010; Rheims et al., 2009). It is highly unlikely that neurons of the isolated embryonic spinal cord exhibit depolarizing GABAergic transmission or SNA due to a deficiency in energy substrates of the saline solution. First, spinal SNA recorded *in vitro* is quite similar to SNA recorded in ovo, as determined by EMG recordings (Landmesser and O'Donovan, 1984; O'Donovan et al., 1998). Second, blockade of $GABA_A$ receptors in vivo (injection of gabazine or bicuculline *in ovo*) blocks embryonic movements suggesting GABAergic currents are likely to be depolarizing in the living embryo (Wilhelm and Wenner, 2008).

Synaptic scaling of GABAergic mPSCs was demonstrated in visual cortical cells in culture, but was not dependent on changes in chloride reversal potential (Kilman et al., 2002). The distinct mechanisms underlying GABAergic scaling in embryonic motoneurons where GABA is excitatory, and cultured cells where GABA is inhibitory could be due to the difference in developmental stages. On the other hand, another study using hippocampal cultures, where GABA was inhibitory, suggested the possibility that inhibitory reversal potential had changed as a compensation to activity blockade, although quantal amplitude was not assessed and E_{GABA} was not directly measured (Karmarkar and Buonomano, 2006). Several other studies have described fast forms of GABAergic synaptic plasticity, involving

shifts in E_{GABA} through changes in the function of Cl^- transporters, although these forms of plasticity are distinct from homeostatic plasticity (Fiumelli and Woodin, 2007; Xu et al., 2008; Yang et al., 2010).

It is becoming clear that the nervous system modulates the strength of inhibition through changes in the regulation of intracellular chloride both in development when intracellular chloride levels are high, and in mature neurons following injury or disease where low chloride levels are increased toward developmental concentrations (Ben-Ari et al., 2007; Blaesse et al., 2009; Fiumelli and Woodin, 2007). Spinal cord injury, nerve injury, traumatic brain injury, axotomy, and ischemia all lead to a pathophysiology that results from a depolarization of E_{GABA} via chloride accumulation (Ben-Ari et al., 2007; Blaesse et al., 2009; Boulenguez et al., 2010; De Koninck, 2007). We have observed a similar response following activity-blockade, as a homeostatic mechanism of GABAergic synaptic scaling. It is therefore tempting to speculate that injury-induced increases in chloride accumulation may be caused by alterations in network activity that trigger homeostatic plasticity mechanisms.

We have previously demonstrated that reduced $GABA_A$ transmission triggers homeostatic changes in synaptic scaling and cellular excitability (Wilhelm et al., 2009; Wilhelm and Wenner, 2008). It will therefore be important in future studies to determine if shifts in E_{Cl} are triggered by $GABA_A$ blockade

Acknowledgments

This research was supported by National Institute of Neurological Disorders and Stroke Grant NS046510 and National Science Foundation Grant 0616097 to P. Wenner and by the Intramural Program of the National Institutes of Neurological Disorders and Stroke. We would like to thank Drs. Michael O'Donovan and Mark Rich for their comments on the manuscript, and Dr. Porfirio Nava for assistance with Western blots.

Bibliography

Ben-Ari Y. Developing networks play a similar melody. Trends Neurosci 2001;24:353–360. [PubMed: 11356508]

Ben-Ari Y, Gaiarsa JL, Tyzio R, Khazipov R. GABA: a pioneer transmitter that excites immature neurons and generates primitive oscillations. Physiol Rev 2007;87:1215–1284. [PubMed: 17928584]

Blaesse P, Airaksinen MS, Rivera C, Kaila K. Cation-chloride cotransporters and neuronal function. Neuron 2009;61:820–838. [PubMed: 19323993]

Boulenguez P, Liabeuf S, Bos R, Bras H, Jean-Xavier C, Brocard C, Stil A, Darbon P, Cattaert D, Delpire E, et al. Down-regulation of the potassium-chloride cotransporter KCC2 contributes to spasticity after spinal cord injury. Nat Med 2010;16:302–307. [PubMed: 20190766]

Chub N, Mentis GZ, O'Donovan M J. Chloride-sensitive MEQ fluorescence in chick embryo motoneurons following manipulations of chloride and during spontaneous network activity. J Neurophysiol 2006;95:323–330. [PubMed: 16192339]

Chub N, O'Donovan MJ. Post-episode depression of GABAergic transmission in spinal neurons of the chick embryo. J Neurophysiol 2001;85:2166–2176. [PubMed: 11353031]

De Koninck Y. Altered chloride homeostasis in neurological disorders: a new target. Curr Opin Pharmacol 2007;7:93–99. [PubMed: 17182282]

Delpy A, Allain AE, Meyrand P, Branchereau P. NKCC1 cotransporter inactivation underlies embryonic development of chloride-mediated inhibition in mouse spinal motoneuron. J Physiol 2008;586:1059–1075. [PubMed: 18096599]

Fiumelli H, Woodin MA. Role of activity-dependent regulation of neuronal chloride homeostasis in development. Curr Opin Neurobiol 2007;17:81–86. [PubMed: 17234400]

Gonzalez-Islas C, Chub N, Wenner P. NKCC1 and AE3 appear to accumulate chloride in embryonic motoneurons. J Neurophysiol 2009;101:507–518. [PubMed: 19036864]

Gonzalez-Islas C, Wenner P. Spontaneous Network Activity in the Embryonic Spinal Cord Regulates AMPAergic and GABAergic Synaptic Strength. Neuron 2006;49:563–575. [PubMed: 16476665]

Hamburger V, Hamilton HL. A series of normal stages in the development of the normal chick embryo. J Morphol 1951;88:49–92.

Hess P, Lansman JB, Tsien RW. Calcium channel selectivity for divalent and monovalent cations. Voltage and concentration dependence of single channel current in ventricular heart cells. J Gen Physiol 1986;88:293–319. [PubMed: 2428919]

Holmgren CD, Mukhtarov M, Malkov AE, Popova IY, Bregestovski P, Zilberter Y. Energy substrate availability as a determinant of neuronal resting potential, GABA signaling and spontaneous network activity in the neonatal cortex in vitro. J Neurochem 2010;112:900–912. [PubMed: 19943846]

Karmarkar UR, Buonomano DV. Different forms of homeostatic plasticity are engaged with distinct temporal profiles. Eur J Neurosci 2006;23:1575–1584. [PubMed: 16553621]

Kilman V, van Rossum MC, Turrigiano GG. Activity deprivation reduces miniature IPSC amplitude by decreasing the number of postsynaptic GABA(A) receptors clustered at neocortical synapses. J Neurosci 2002;22:1328–1337. [PubMed: 11850460]

Landmesser LT, O'Donovan MJ. Activation patterns of embryonic chick hind limb muscles recorded in ovo and in an isolated spinal cord preparation. J Physiol (Lond) 1984;347:189–204. [PubMed: 6707956]

O'Donovan MJ. The origin of spontaneous activity in developing networks of the vertebrate nervous system. Curr Opin Neurobiol 1999;9:94–104. [PubMed: 10072366]

O'Donovan MJ, Chub N, Wenner P. Mechanisms of spontaneous activity in developing spinal networks. J Neurobiol 1998;37:131–145. [PubMed: 9777737]

Rheims S, Holmgren CD, Chazal G, Mulder J, Harkany T, Zilberter T, Zilberter Y. GABA action in immature neocortical neurons directly depends on the availability of ketone bodies. J Neurochem 2009;110:1330–1338. [PubMed: 19558450]

Rich MM, Wenner P. Sensing and expressing homeostatic synaptic plasticity. Trends Neurosci 2007;30:119–125. [PubMed: 17267052]

Turrigiano GG. The self-tuning neuron: synaptic scaling of excitatory synapses. Cell 2008;135:422–435. [PubMed: 18984155]

Turrigiano GG, Leslie KR, Desai NS, Rutherford LC, Nelson SB. Activity-dependent scaling of quantal amplitude in neocortical neurons. Nature 1998;391:892–896. [PubMed: 9495341]

Vinay L, Jean-Xavier C. Plasticity of spinal cord locomotor networks and contribution of cation-chloride cotransporters. Brain Res Rev 2008;57:103–110. [PubMed: 17949820]

Wilhelm JC, Rich MM, Wenner P. Compensatory changes in cellular excitability, not synaptic scaling, contribute to homeostatic recovery of embryonic network activity. Proc Natl Acad Sci U S A 2009;106:6760–6765. [PubMed: 19346492]

Wilhelm JC, Wenner P. GABAA transmission is a critical step in the process of triggering homeostatic increases in quantal amplitude. Proc Natl Acad Sci U S A 2008;105:11412–11417. [PubMed: 18678897]

Wilson NR, Kang J, Hueske EV, Leung T, Varoqui H, Murnick JG, Erickson JD, Liu G. Presynaptic regulation of quantal size by the vesicular glutamate transporter VGLUT1. J Neurosci 2005;25:6221–6234. [PubMed: 15987952]

Xu C, Zhao MX, Poo MM, Zhang XH. GABA(B) receptor activation mediates frequency-dependent plasticity of developing GABAergic synapses. Nat Neurosci 2008;11:1410–1418. [PubMed: 18953347]

Yang B, Tadavarty R, Xu JY, Sastry BR. Activity-mediated plasticity of GABA equilibrium potential in rat hippocampal CA1 neurons. Exp Neurol 2010;221:157–165. [PubMed: 19879261]

Zhang LI, Poo MM. Electrical activity and development of neural circuits. Nat Neurosci 2001;4(Suppl):1207–1214. [PubMed: 11687831]

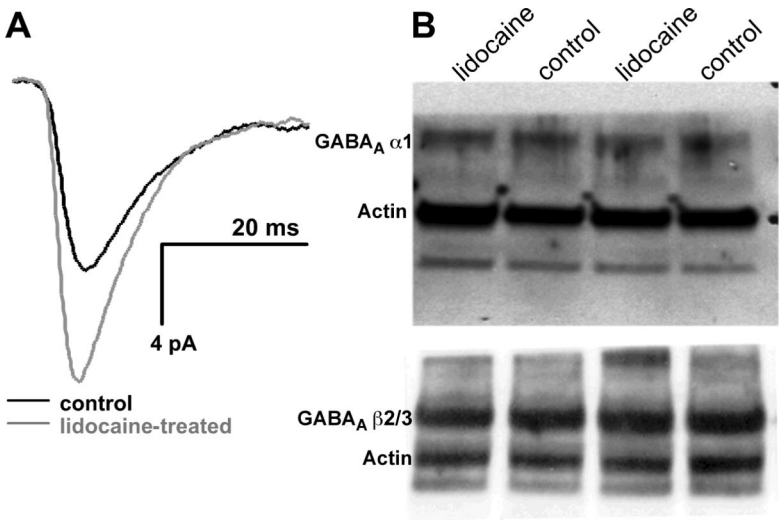

Figure 1.

Activity-blocked motoneurons have increased GABAergic mPSC amplitude that do not appear to be mediated by changes in total protein levels of $GABA_A$ subunits. A) $GABA_A$ mPSC amplitude was increased in activity-blocked motoneurons compared to controls, as shown in the averaged trace. B) Western blots from control and activity-blocked ventral spinal cords demonstrate no difference in total protein of either α1 or β2/3 $GABA_A$ subunits (normalized to actin protein levels).

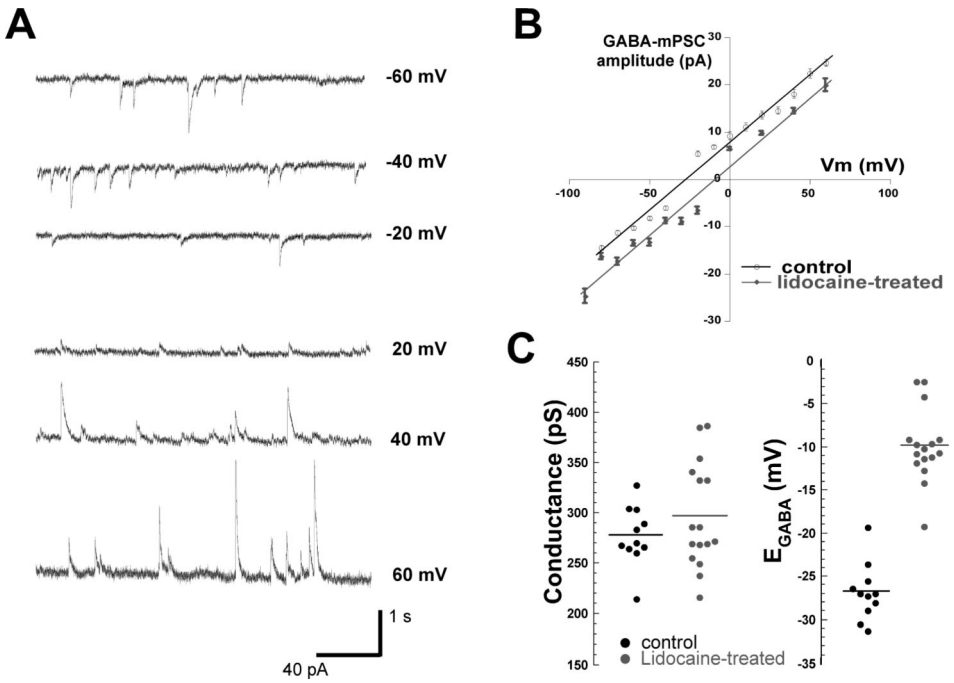

Figure 2.

I_{mPSC}-V plots from motoneurons show that GABAergic mPSC conductance was no different in control and treated embryos, while E_{GABA} was depolarized. A) mPSCs are shown at voltage steps of 20 mV increments in a motoneuron from an activity-blocked embryo. B) The average amplitude of GABAergic mPSCs at each step were then plotted against the step voltage. The graph is the average from all control and activity-blocked motoneurons. Error bars represent SE. C) Plots show GABAergic mPSC conductance (left) and reversal potentials (right) for several recorded cells (dots) from control (black) and activity-blocked (grey) embryos. Black line represents average values for cells.

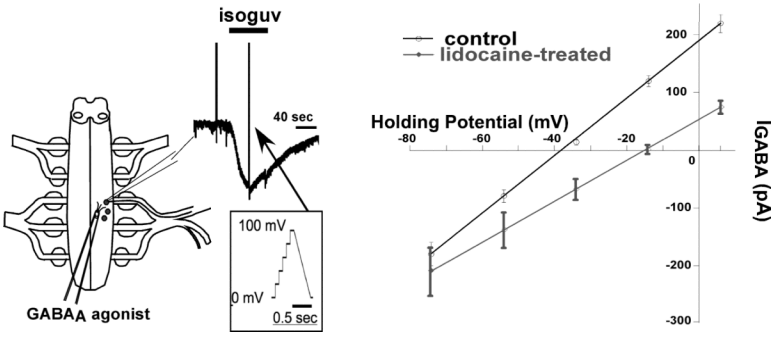

Figure 3.

Perforated patch recordings show a depolarizing shift in GABAergic reversal potential in motoneurons from activity-blocked embryos. Schematic shows puffing electrode adjacent to whole cell recorded motoneuron. Trace shown of voltage clamp recording using perforated patch electrode while picospritzing a $GABA_A$ agonist (isoguvacine, −60mV). Two voltage ramps are applied (one before and the other during agonist application). Box expands image of ramp, which is composed of upward steps followed by a downward ramp. GABAergic I–V plots of control and activity-blocked motoneurons were generated by subtracting plots (isoguvacine - baseline). Plots are an average from 7 control and 7 activity-blocked embryos. Error bars represent SE.

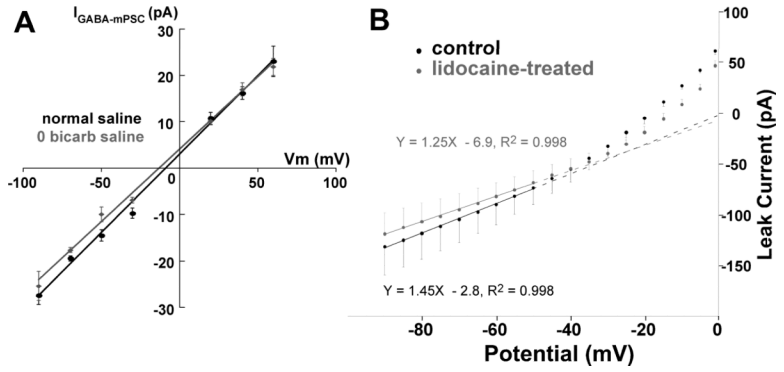

Figure 4.

The shift in E_{GABA} was mediated by an increase in Cl^- accumulation. A) The shift in E_{GABA} was not mediated by a change in $GABA_A$ receptor HCO_3^- permeability. An I_{mPSC}-V plot does not show significant shifts in E_{GABA} before and after perfusing a 0mM HCO_3^- extracellular solution (average of 4 cells). B) Enhanced Cl^- accumulation in activity-blocked embryos was not due to changes in Cl^- leak current. I–V plot constructed of a ramp from 0mV to −90mV. A linear fit of the data was made (−50 to −90mV). Cl^- conductance was not significantly different in control and activity-blocked embryos. Equations for fitted lines are shown, and these lines are extended (dashed line) to approximate the currents reversal potential. Error bars represent SE.